JOURNAL OF MATERIALS SCIENCE 23 (1988) 3864-3868

Analysis of static and dynamic fatigue of polycrystalline alumina

K. K. PHANI
Central Glass and Ceramic Research Institute, Calcutta 700 032, India

The fatigue failure of polycrystalline alumina in a moist air environment at 30° C has been analysed in terms of a modified Weibull distribution function using fracture mechanics theory. The good correlation obtained between the fatigue test data and fracture mechanics theory indicates that fatigue is controlled by the slow crack growth of pre-existing flaws. The distribution of these pre-existing flaws can be represented by the modified Weibull distribution which provides an upper and a lower limit strength and thus is more realistic for the physical phenomena it represents. Comparison of proof-test predictions with experiment indicate that the proof test can be effective in eliminating weak samples from the population.

1. Introduction

Ceramic materials are finding increasing use in high performance, structural application. However, a problem in their utilization is to ensure mechanical reliability and safety. Two factors that complicate design for their mechanical reliability are delayed failure, commonly known as static fatigue, and a wide variability in fracture strength due to their brittle nature. To make failure predictions for glass and ceramic materials, a fundamental theory has been developed from fracture mechanics principles [1–4]. This theory is based on the assumption that fatigue failure occurs by the stress-dependent growth of pre-existing flaws to dimensions critical for spontaneous crack propagation. On the other hand, scatter in strength which is attributed to scatter in initial flaw sizes, is usually analysed in terms of the "weakest link theory" which is based on the theory that the fracture is controlled by the weakest defect of all the defects present in a system. The form of the weakest link theory commonly applied to ceramic materials is that to Weibull [5]. Thus, Weibull analysis combined with fracture mechanics principles forms the probabilistic basis for the design of ceramic materials. Although the fracture mechanics principles provide a sound basis for fatigue failure predictions, difficulties are encountered in analysing the strength distribution in terms of Weibull distribution. Several investigators [6–10] have reported that, as predicted by theory, the strength data when plotted on a Weibull probability graph, do not yield a straight line. As an alternative approach, a bimodal Weibull analysis has been used for the analysis of data from the view point that the distribution is controlled by more than one type of flaw population. Ritter and Humenik [7] have reported a similar analysis for the strength data on polycrystalline alumina, although they could not identify the origin of the flaw responsible for two strength populations. A modified Weibull distribution function for analysing the strength data of ceramic materials has been proposed [11, 12].

The purpose of this paper is to determine the applicability of this modified function along with fracture mechanics theory in predicting fatigue failure of polycrystalline alumina under various loading conditions. Theoretical predictions regarding the probability of fatigue failure before and after proof testing have also been compared with the experimental data reported by Ritter and Humenik [7].

2. Analytical procedure

2.1. Fatigue failure

The fatigue effect on ceramic materials is usually determined by measuring the time to failure as function of applied stress and by measuring the dependence of fracture strength on stressing rate. These experimental techniques are usually known as static and dynamic fatigue, respectively.

Based on a single power-law relationship between the subcritical crack velocity and the stress intensity factor, the time to failure (t_f) at a constant applied tensile stress (σ_a) is given by [1, 2]

$$t_f = BS_i^{N-2}\sigma_a^{-N} \quad (1)$$

where S_i is the fracture strength in an inert environment and B, N are crack growth constants for a given material and environment. Similarly, the fracture strength (S) at a constant stressing rate ($\dot{\sigma}$) is given by [2, 13]

$$S^{N+1} = B(N+1)S_i^{N-2}\dot{\sigma} \quad (2)$$

Assuming that the origin of fracture is the same for both fatigue and inert failures, the probability of failure (F) for a given t_f and σ_a (or a given S and $\dot{\sigma}$) can be obtained from Equation 1 (or Equation 2) by expressing the inert strength in terms of its failure probability distribution.

0022–2461/88 $03.00 + .12

2.2. Probability distribution function

The failure analysis of brittle solids is usually based on the Weibull distribution function given by

$$F = 1 - \exp[-(S/S_0)^m] \quad (3)$$

where F is the probability of failure at a stress S or below, S_0 and m are the scaling parameter and Weibull modulus, respectively. Equation 3 shows that a plot of $\ln\ln[1/(1-F)]$ against $\ln S$ should yield a straight line. Such a plot for the strength data on polycrystalline alumina, reported by Ritter and Humenik [7] is shown in Fig. 1. The data points lie on a smooth curve rather than on a straight line. From the lack of linearity of such plots for extensive data reported in the literature [6, 14–18] it has been concluded [15] that Weibull distribution is not applicable to the entire strength distribution. As an alternative approach, a bimodal Weibull distribution is usually used for the analysis of strength data, though strict application of the distribution presumes a single mode of failure [16]. Snowden [16] has analysed the statistical justification for using a bimodal Weibull distribution and concluded that the beta distribution, rather than the Weibull distribution, describes the data best. In the beta distribution, the values of the variate are limited to a finite interval, which is more realistic for the strength of brittle materials. It has also two shape parameters. On the other hand, for certainty of failure, Weibull distribution requires $S = \infty$, which is a physically unsatisfactory boundary condition. To overcome this limitation, a modification [11, 12] of Equation 3 has been proposed in the form

$$F = 1 - \exp\{[(S - S_L)/S_0]^{m_1}[(S_u - S)/S_{0_2}]^{m_2}\} \quad (4)$$

where S_L and S_u are the lower and upper strength limit of the material, S_{0_1}, S_{0_2} and m_1, m_2 are the two location and shape parameters, respectively. Equation 4 can be expressed in the form

$$\ln\ln[1/(1-F)] = m_1\ln[(S - S_L)/S_{0_1}] - m_2\ln[(S_u - S)/S_{0_2}] \quad (5)$$

which shows, depending on the parameter values, a plot of $\ln\ln[1/(1-F)]$ against $\ln S$ will be a smooth curve.

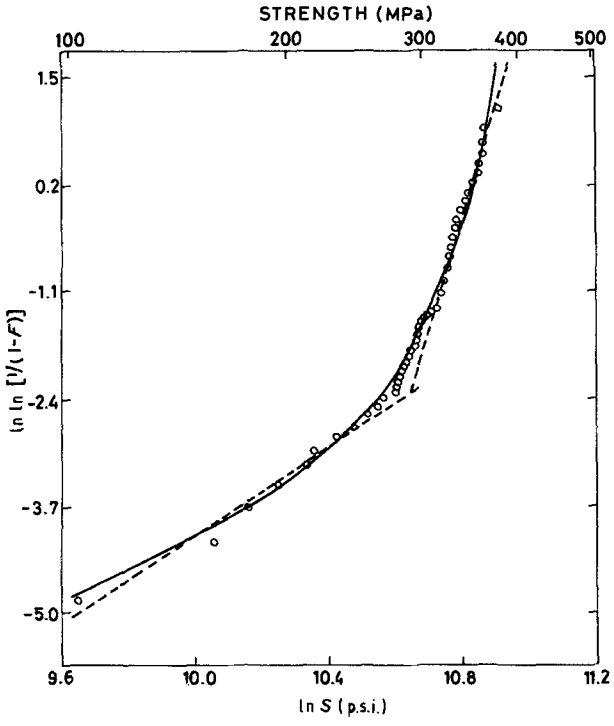

Figure 1 Weibull plot of strength distribution of polycrystalline alumina in ambient air (22° C, 70% r.h.) for a stressing rate of 2000 p.s.i. sec^{-1}.

2.3. Proof testing

The proof testing of ceramics is carried out to eliminate the weak samples from the population so that the after-proof strength distribution will be stronger than the initial distribution. By considering crack growth during loading but not unloading, Evans and Wiederhorn [1] have shown that the inert strength (S_i') after proof testing is given by

$$(S_i'/S_i)^{N_p-2} = 1 - (\sigma_p^*/S_i)^{N_p-2}[1 - (\sigma_p/\sigma_p^*)^{N_p-2}] \quad (6)$$

where N_p is the fatigue parameter for the proof test conditions, S_i is the inert strength before proof test and σ_p^* is the equivalent proof stress for inert conditions, i.e. the proof stress for an inert proof test environment having the same probability of failure as that of σ_p in the actual proof test environment. The failure probability after proof test (F_a) is related to the initial failure probability (F) by [1]

$$F_a = (F - F_p)/(1 - F_p) \quad (7)$$

where F_p is the failure probability of the proof test. Thus for a given N_p, σ_p and F_p, the after-proof-test inert strength distribution can be calculated from Equations 6 and 7 and the initial inert strength distribution.

3. Data analysis and discussion

As mentioned earlier, the fatigue strength data on polycrystalline alumina, reported by Ritter and Humenik [7] has been used in the following analysis. The specimens used by them were alumina bars sintered at 1550° C and containing about 10% alkaline earth, aluminosilicate glassy phase with average grain size 4 to 5 μm. The static and dynamic fatigue tests were carried out in a controlled air environment of 30 ± 5% r.h. using a four-point bend test, having an inner span of 0.625 in. (15.875 mm). Six different stress levels were used for static fatigue and dynamic fatigue was measured at four different stressing rates. In addition, a group of samples were proof tested in ambient air (22° C and 70% r.h.) at a stress of 45 000 p.s.i. (10^3 p.s.i. = 6.89 N mm^{-2}). One group of 25 proof-tested samples were tested in liquid nitrogen for inert strength and the other two groups were subjected to

TABLE I Fatigue parameters for polycrystalline alumina in moist air at 30° C [7]

Test technique	N	log B (p.s.i.^{2} sec)
Static fatigue	37.70	2.72
Dynamic fatigue	35.53	3.44

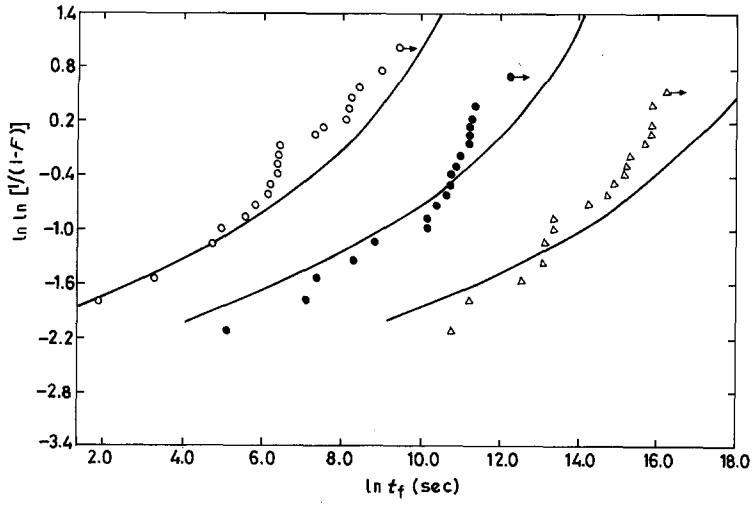

Figure 2 Comparison of the time-to-failure data for polycrystalline alumina in moist air (80% r.h.) at 30° C to that predicted (——) from Equation 1 coupled with Equation 9 with $N = 37.7$ and $\log B = 2.72$ p.s.i.^{2} sec. σ_a = (○) 35 909, (●) 32 567, (△) 28 500 p.s.i.

static fatigue test at applied stresses of 30 000 and 27 350 p.s.i. Also the fracture strength of another 126 samples was measured in ambient air (22° C, 70% r.h.) at stressing rate of 2000 p.s.i. sec^{-1}. The values of parameters N and B as determined by Ritter and Humenik [7] from the analysis of static and dynamic fatigue data are given in Table 1. These values have been used in subsequent analysis.

Fig. 1 shows a plot of fracture strength of specimens tested in ambient air at stressing rate of 2000 p.s.i. sec^{-1} on Weibull axes. For fitting Equation 5 to the data, initial estimates of S_L and S_u were taken as experimentally measured lowest and highest strength values, respectively. A set of values were assumed for S_{01} and S_{02} and the values of m_1 and m_2 were determined by regression analysis of data. From the calculated and experimental values of $\ln\ln[1/(1 - F)]$, a least squares sum was evaluated for the particular set of parameters S_{01} and S_{02}. The computation was then iterated with a new set of S_{01} and S_{02} until the minimum least squares sum was obtained. The procedure was repeated by changing the values of S_u and S_L, again using the minimum least squares sum as the criteria for best fitted distribution, obtained thus, is

$$\ln\ln[1/(1 - F)] = 0.10\ln[(S - 15\,000)/78\,000] - 2.87\ln[(60\,000 - S)/10\,000] \quad (8)$$

The equation is shown by a solid line in Fig. 1. As can be seen from the figure, it shows excellent agreement with the data. As a measure of goodness of fit between the data and the fitted Equation 8, the sum of squares was evaluated from the expression

$$Q = 1 - \sum_{j=1}^{n} (S_j - \hat{S}_j)^2 / \sum_{j=1}^{n} (S_j - \bar{S})^2 \quad (9)$$

where $\hat{S}_j$ is the value of failure stress calculated for the appropriate F value from the ranking of failure strengths and calculated parameters of the distribution function; S_j is the measured strength values and $\bar{S}$ is the mean of the distribution. The value of Q was obtained as 0.992, again indicating excellent agreement between the data and the fitted equation. It may be noted that Ritter and Humenik [7] fitted two Weibull distributions, as shown by dotted lines in Fig. 1, to the data on the assumption that the low strength flaws were a result of gross damage incurred in grinding the samples. However, their attempts to identify the fracture origin in these samples failed.

Based on the strength distribution given by Equation 8, the inert strength distribution was determined using Equation 2 and the appropriate parameter values given in Table I to be,

$$\ln\ln[1/(1 - F)] = 0.24\ln[(S - 19\,000)/69\,000] - 2.21\ln[(78\,000 - S)/10\,000] \quad (10)$$

Figs 2 to 4 compare the experimental results on the probability of fatigue failure with that predicted from Equations 1 and 2 using the inert strength distribution given by Equation 10. In general, there is good agreement between the predicted and measured distribution except for the low-strength values in the dynamic fatigue experiment. This is possibly due to the reason that the comparison is based on 25 samples, which is insufficient to define the low-strength population. It may be mentioned that Ritter and Humenik [7] reported failures on loading for the static fatigue test

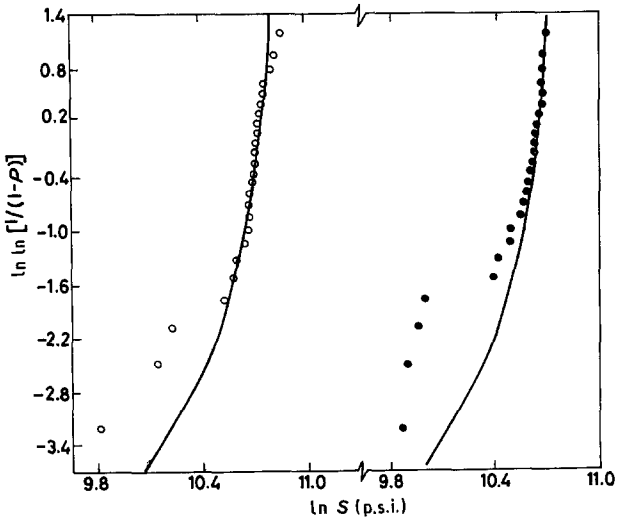

Figure 3 Comparison of dynamic fatigue data for polycrystalline alumina at stress rate (●) 20 and (○) 200 p.s.i. sec^{-1} in moist air at 30° C to that predicted (——) from Equation 2 coupled with Equation 9 with $N = 37.53$ and $\log B = 3.44$ p.s.i.^{2} sec.

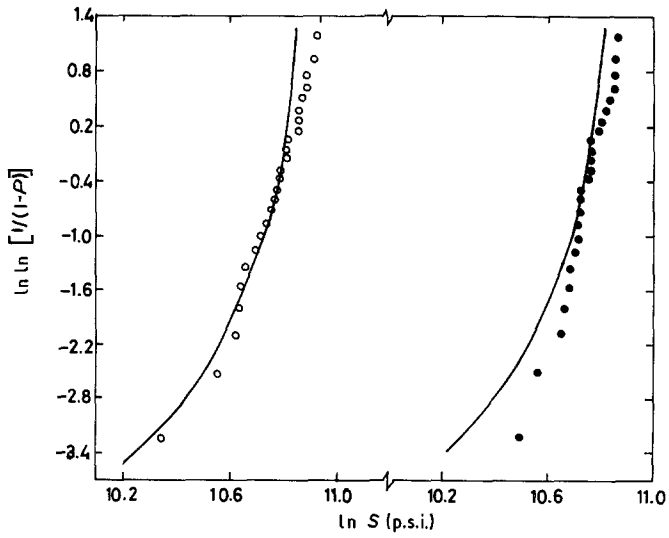

Figure 4 Comparison of dynamic fatigue data for polycrystalline alumina at stress rate (●) 2000 and (○) 10 000 p.s.i. sec^{-1} in moist air (50% r.h.) at 30° C to that predicted (——) from Equation 2 coupled with Equation 9 with $N = 37.53$ and $\log B = 3.44$ p.s.i.^{2} sec.

at 35 909 p.s.i. The inert strength value corresponding to the probability of failure of the third sample is estimated to be about 54 176 from Equation 10 and the corresponding time to failure at 35 909 p.s.i. is obtained as 1.4 sec from Equation 1, indicating almost instantaneous failure on loading. Thus this provides further evidence of agreement between theory and experimental results.

In Fig 5 the inert strength distribution after proof testing in ambient air is compared to the initial inert strength distribution and to that predicted theoretically from Equation 6. For the proof stress of 45 000 p.s.i., F_p was estimated to 0.287 and the corresponding σ_p^* was obtained as 65 294.7 p.s.i. from Equation 10. N_p was taken to be equal to that measured in fatigue tests, 37.6. Good agreement is apparent between theory and experiment and it is evident that proof testing was effective in eliminating the weak specimens from the population.

The lifetime after proof testing (t_f) is obtained from Equation 1 by replacing t_f and S_i,

$$t_f' = B(S_i')^{N-2}\sigma_a^{-N} \quad (11)$$

Fig. 6 compares the after-proof failure time distribution at 30 000 p.s.i. to that predicted from Equation 11. Although the data of only nine samples have been reported, it is seen that the predicted after-proof lifetimes are in reasonable agreement with experiment.

4. Conclusions

1. The probability of fatigue failure of polycrystalline alumina has been analysed in terms of a modified Weibull distribution along with fracture mechanics theory. The good agreement between the predicted and experimental values indicates that fatigue failure of alumina occurs by the subcritical crack growth of pre-existing flaws and the distribution of these pre-existing flaws can be represented by the modified Weibull distribution given by Equation 5.

2. The modified Weibull distribution provides an

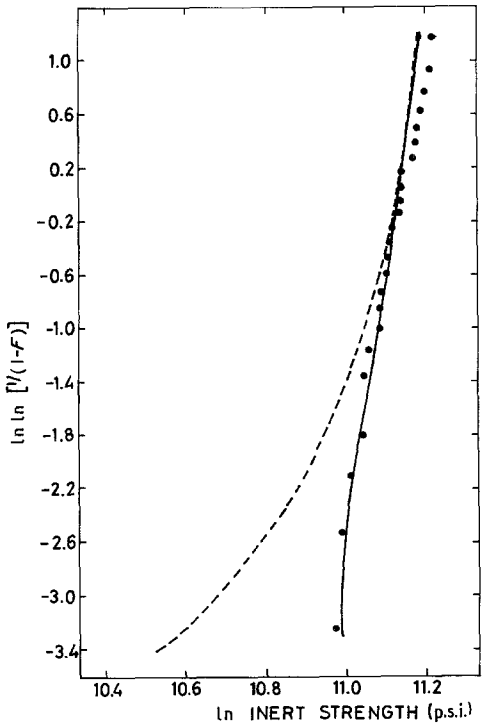

Figure 5 Inert strength distribution of polycrystalline alumina (- - -) before and (●) after proof testing in air compared to (——) the predicted after proof strength distribution given by Equation 6 where $\sigma_p = 45\,000$ p.s.i., $N_p = 37.6$, $F_p = 0.287$ and $\sigma_p^* = 65\,294.7$ p.s.i.

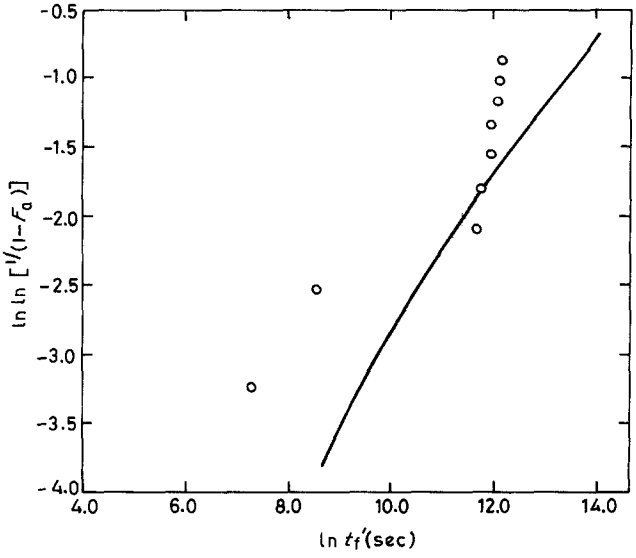

Figure 6 Comparison of the after-proof failure time distribution at $\sigma_a = 30\,000$ p.s.i. of polycrystalline alumina in moist air to that predicted from Equation 10 with $N = 37.7$, $\log B = 2.72$ p.s.i.^{2} sec, $F_p = 0.16$ and $\sigma_p^* = 57\,360.97$ p.s.i.

upper and a lower strength limit and is therefore more realistic in defining the strength of brittle materials.

3. Proof testing of polycrystalline alumina in ambient air can be effective in eliminating weak samples from the initial distribution.

Acknowledgements

The author thanks Dr S. Kumar, Director of the Institute for his kind permission to publish this paper. Thanks are due to Shri S. Sengupta for preparation of the line diagrams of this paper.

References

1. A. G. EVANS and S. M. WIEDERHORN, *Int. J. Fract.* **10** (1974) 379.
2. J. E. RITTER Jr, in "Fracture Mechanics of Ceramics", Vol. 4, edited by R. C. Bradt, D. P. H. Hasselman and F. F. Lange (Plenum, New York, 1978) p. 667.
3. J. E. RITTER Jr and J. A. MEISEL, *J. Amer. Ceram. Soc.* **59** (1976) 478.
4. R. W. DAVIDGE, J. R. McLAREN and G. TAPPIN, *J. Mater. Sci.* **8** (1973) 1699.
5. W. WEIBULL, *J. Appl. Mech.* **18** (1951) 293.
6. G. K. BANSEL and W. H. DUCKWORTH, in "Fracture Mechanics of Ceramics", Vol. 3, edited by R. C. Bradt, D. P. H. Hasselman and F. F. Lange (Plenum, New York, 1978) p. 201.
7. J. E. RITTER Jr and J. N. HUMENIK, *J. Mater. Sci.* **14** (1979) 626.
8. K. GODA and H. FUKUNAGA, *ibid.* **21** (1986) 4475.
9. P. MARTINEAU, M. LAHAYE, R. PAILLER, R. NASLAIN, M. COUZI and F. CRUEGE, *ibid.* **19** (1984) 2731.
10. T. E. EASLER, R. C. BRADT and R. E. TRESSLER, *J. Amer. Ceram. Soc.* **64** (1981) 731.
11. K. K. PHANI, *ibid.* **70** (1987) c182.
12. *Idem, J. Appl. Phys.*, **62** (1987) 719.
13. A. G. EVANS, *Int. J. Fract.* **10** (1974) 251.
14. R. D. MAURER, *Appl. Phys. Lett.* **27** (1975) 220.
15. D. KALISH, B. K. TARIYAL and R. O. PICKWICK, *Amer. Ceram. Soc. Bull.* **56** (1977) 451.
16. W. E. SNOWDEN, in "Fracture Mechanics of Ceramics", Vol. 3, edited by R. C. Bradt, D. P. H. Hasselman and F. F. Lange (Plenum, New York, 1978) p. 143.
17. W. D. SCOTT and A. GADDIPATTI, *ibid.*, p. 125.
18. B. K. TARIYAL and D. KALISH, *Mater. Sci. Engng* **27** (1977) 69.

Received 23 June 1987
and accepted 11 January 1988